Viscoelastic Synergy in Aqueous Mixtures of Wormlike Micelles and Model Amphiphilic Triblock Copolymers

Tomohide Yoshida, Rajiv Taribagil, Marc A. Hillmyer,* and Timothy P. Lodge*

Departments of Chemistry and Chemical Engineering & Materials Science, University of Minnesota, Minneapolis, Minnesota 55455-0431

Received October 20, 2006; Revised Manuscript Received December 5, 2006

ABSTRACT: We explored the rheological consequences of adding low concentrations of model hydrophobically end-capped poly(ethylene oxide)s to aqueous solutions containing 1 wt % cetyltrimethylammonium tosylate, a surfactant well recognized to form wormlike micelles with hydrophobic alkyl cores. We describe the synthesis and characterization of a variety of hydrophobically modified polymers and report the linear viscoelastic moduli and steady shear viscosity for combinations of 1 wt % cetyltrimethylammonium tosylate with the various hydrophobically modified polymers. Addition of as little as 0.1 wt % hydrophobically modified poly(ethylene oxide) leads to a massive enhancement in viscoelastic response that is strongly promoted by increasing hydrophobe length at fixed polymer molecular weight and concentration and also by increasing the poly(ethylene oxide) molecular weight at fixed concentration. From the detailed examination of how polymer concentration, length of hydrophobic sticker, polymer molecular weight, and architecture of the hydrophobically modified polymers influence the rheological properties of these admixtures, we posit a molecular mechanism to explain the enhancement in the viscoelastic response that implicates intercalation of the hydrophobic "stickers" into the wormlike micelles and thus "physically cross-linking" the system.

Introduction

The ability of certain surfactants and surfactant mixtures to form very long, threadlike or wormlike micelles (WLMs) in aqueous solution has been well documented.[1−36] Furthermore, these systems often display extremely rich rheological responses, even at rather modest concentrations; examples include Maxwell-like viscoelasticity, shear thinning, and even rather dramatic shear thickening. These phenomena are being commercially exploited, for example, in detergent and shampoo formulations and in fracturing fluids.[37] Similarly rich rheological phenomena can be obtained with associative thickeners or hydrophobically modified polymers (HMP).[38−42] In these systems a nominally water-soluble polymer is decorated with some number of insoluble "stickers", often simple hydrocarbons, that associate and ultimately lead to gelation. In both cases the interesting rheological properties are traceable to the large size of the assemblies, but the ability of the associations to be disrupted by thermal forces and by flow plays a crucial role. It has recently been reported that a *combination* of WLMs and HMPs can yield greatly enhanced viscoelastic response, at concentrations for which the WLMs and HMPs individually do not.[43−45] This synergy has interesting implications in that rheological control can be achieved using less added material and that rheological response can be manipulated by multiple variables in a given system. However, the underlying mechanism(s) remain to be clarified.

The work to be described herein was motivated by two particular studies, in which specific combinations of WLMs and HMPs (erucyl bis(hydroxyethyl)methylammonium chloride [EHAC] + hydrophobically modified polyacrylamide[43] and EHAC + hydrophobically modified guar,[44] respectively) showed strong synergistic effects. A plausible interpretation of these observations posited by the authors of refs 43 and 44 is that the hydrophobic "stickers" on the HMPs intercalate into the WLMs, thereby acting as physical cross-links (see Figure 1). In both cases the rather ill-defined structure of the HMP may inhibit a more detailed mechanistic understanding. Accordingly, we have undertaken a systematic study using model HMPs. In particular, poly(ethylene oxide) (PEO) serves as the water-soluble polymer and linear alkanes (C_{14}, C_{18}, and C_{22}) as the stickers. We have varied the molecular weight of the PEO from ca. 10^4 to 10^5 g/mol and also the architecture (mono-end-capped "diblock", doubly-end-capped "triblock", and triply-end-capped three-arm star polymers). Aqueous solutions of analogous hydrophobically end-capped PEO chains have been extensively studied.[46−64] The WLM system employed here is cetyltrimethylammonium tosylate (CTAT), at a constant concentration of 1 wt %. CTAT was chosen because of its well-documented ability to form WLMs and because its structure and rheological properties in aqueous solution have also been extensively explored.[13−16,29,30]

The remainder of the paper is organized as follows. First we describe the synthesis and characterization of the diblock, triblock, and three-arm star HMPs. Then we report the linear viscoelastic moduli (G', G'' vs frequency, ω) and steady shear viscosity (η vs shear rate, γ) for combinations of 1% CTAT with the various HMPs and at varying HMP concentration. The enhancement of the viscoelastic response is strongly promoted by increasing hydrophobe length at fixed HMP molecular weight and concentration and also by increasing the PEO molecular weight and fixed concentration. The results are discussed in terms of the qualitative picture implied by the cartoon in Figure 1.

Results

Hydrophobically Modified Polymer Synthesis. The ABA block copolymers used in this study contained PEO as the water-soluble midblock and hydrophobic, long-chain alkyl groups as the water insoluble end "blocks" (stickers). These materials were prepared by the anionic polymerization of ethylene oxide

* Corresponding authors. E-mail: hillmyer@chem.umn.edu, lodge@chem.umn.edu.

10.1021/ma062428+ CCC: $37.00
Published on Web 02/01/2007

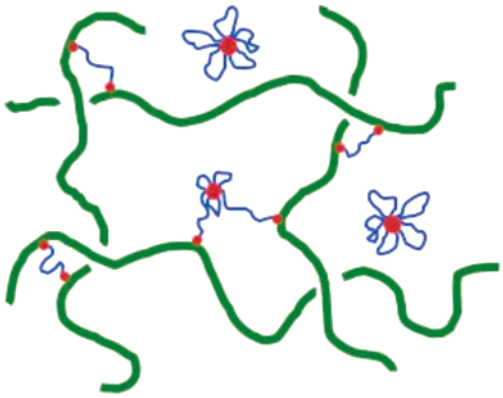

Figure 1. Drawing of WLMs formed from CTAT (green) and hydrophobically end-capped (red groups) PEO (blue).

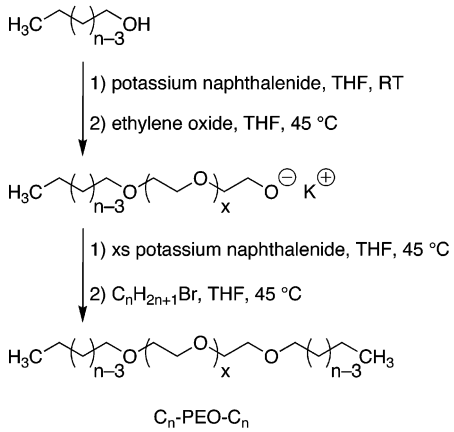

Figure 2. Synthesis of C_n-PEO-C_n ABA triblock copolymers. *n* designates the total number of carbons in alkyl end groups.

initiated by the potassium alkoxide derivative of the alkyl alcohols $C_{14}H_{29}OH$, $C_{18}H_{37}OH$, or $C_{22}H_{45}OH$ formed by titration with the strong base potassium naphthalenide.[65] The polymerizations of ethylene oxide were conducted in THF at 45 °C and terminated by the corresponding alkyl bromides $C_{14}H_{29}Br$, $C_{18}H_{37}Br$, or $C_{22}H_{45}Br$. To ensure high end-capping efficiencies, excess potassium napthalenide was added to the reaction after complete conversion of the ethylene oxide. To generate the corresponding diblock copolymers, the polymerizations were terminated by acidic methanol, thus giving a PEO with only one hydrophobic group. The synthetic scheme is shown in Figure 2. Using this protocol, a series of hydrophobically end-capped PEO materials were prepared and are listed in Table 1 as C_n-PEOzK-C_n, where *n* is the number of carbons in the alkyl end groups and *z* is the molecular weight of the PEO midblock in kg mol^{-1}. The PEO molecular weights were determined by ^{1}H NMR spectroscopy assuming exactly two alkyl end groups per polymer chain. All of the C_n-PEOzK-C_n materials were characterized by relatively narrow molecular weight distributions (PDI $\leq$ 1.3) as determined by SEC.

The three-arm star block copolymers were synthesized using a similar procedure. For these materials the potassium alkoxide of the trifunctional alcohol 1,3,5-cyclohexanetriol was used to initiate the ethylene oxide polymerization. These polymerizations of ethylene oxide were conducted in THF at 45 °C and terminated only by $C_{22}H_{45}Br$. Again, excess potassium naphthalenide was added to the reaction after complete conversion of the ethylene oxide to ensure complete end-capping. The corresponding PEO star homopolymers were produced by termination with acidic methanol. The synthetic scheme is depicted in Figure 3, and the star blocks are listed in Table 1 as C_6(PEOzK-C_{22})$_3$, where *z* is the molecular weight of the PEO midblock in kg mol^{-1}. The PEO molecular weights were determined by ^{1}H NMR spectroscopy assuming exactly three alkyl end groups per polymer chain. The two star block copolymers gave PDIs < 1.4 as determined by SEC.

Sample Preparation. All of the aqueous solutions used in this study were prepared by mixing the polymers and CTAT with water in a sealed vial at 60 °C for 24 h. The solutions were then cooled to RT and stored for at least 24 h before rheological analysis. Dynamic and steady rheological measurements were carried out using a Rheometrics RFS II rheometer equipped with a cup-and-bob geometry (see Experimental Details).

Steady Flow and Viscoelastic Behavior of CTAT/Polymer Mixtures. The viscosity profiles of a 1 wt % CTAT solution and an 0.1 wt % solution of C_{18}-PEO94K-C_{18} as a function of shear rate ($\dot{\gamma}$) at 25 °C are shown in Figure 4. Extrapolation to the Newtonian plateau at low shear rates gives values of the zero-shear viscosity η_0 for these two solutions of 0.2 and 0.001 Pa·s, respectively. Clearly, the C_{18}-PEO94K-C_{18} solution is only slightly more viscous than water, as expected for a rather dilute solution of spherical micelles (the assumed structure), and it exhibits Newtonian behavior over the experimentally accessible range of shear rates. In contrast, the 1 wt % CTAT solution has a considerably higher viscosity. This particular concentration is just above the regime where strong shear thickening has been reported[30,39] but is not high enough to be substantially entangled (vide infra). The CTAT solution also shows a crossover to shear thinning behavior at about 10 s^{-1}. The solution containing both 0.1 wt % C_{18}-PEO94K-C_{18} and 1 wt % CTAT exhibits massive enhancement in η_0 to nearly 20 Pa·s (Figure 4). On the other hand, addition of 0.1 wt % C_{18}-PEO94K-OH (the synthetic diblock precursor to the triblock C_{18}-PEO94K-C_{18}) to a 1 wt % CTAT solution led to a small *decrease* in η_0 compared to the pure 1 wt % CTAT solution (data not shown). The crossover to shear thinning behavior for the C_{18}-PEO94K-C_{18}/CTAT mixture occurs at lower shear rates (ca. 0.5 s^{-1}) relative to the pure CTAT solution. The steady shear behavior for the 1 wt % CTAT solutions containing 0.1 wt % C_{18}-PEO14K-C_{18}, C_{18}-PEO30K-C_{18}, or C_{18}-PEO47K-C_{18} are also shown in Figure 4, and the zero-shear viscosity behavior for this series of 0.1 wt % block copolymer/1 wt % CTAT solutions is summarized in Figure 5. As the PEO midblock molecular weight is lowered, the viscosity enhancement is also reduced; in fact, for the lowest molecular weight (C_{18}-PEO14K-C_{18}) the viscosity of the solution is less than that of the CTAT alone. Analogous solutions at constant hydrophobic sticker concentration (ca. 0.02 mM) as opposed to constant polymer weight concentration were prepared, and the zero-shear viscosity behavior for those solutions is also shown in Figure 5. With the exception of the solution containing C_{18}-PEO14K-C_{18}, the addition of the low levels of the C_n-PEO-C_n triblocks to 1 wt % CTAT solutions results in significant increases in η_0 that depend on the molecular weight of the triblock.

The frequency-dependent elastic (G') and loss (G'') moduli for the 1 wt % CTAT solution at 25 °C are shown in Figure 6. This solution has a characteristic relaxation time (τ_R) of 0.05 s, as determined by the crossover frequency (ω_c) at which the G' and G'' values are equal, $\tau_R = \omega_c^{-1}$. Addition of 0.1 wt % C_{18}-PEO94K-OH to the solution has little discernible influence on the viscoelastic response in general, or on τ_R in particular, although a small decrease in relaxation time and viscosity can be resolved (Figure 6). We were unable to measure the dynamic

Table 1. Molecular Characteristics of End-Alkylated Poly(ethylene oxide) Samples

sample code	architecture	$M_n \times 10^{-3}$ [a]	M_w/M_n [a]	[EO]/[C] [b]	PEO $M_n \times 10^{-3}$ [c]
C_{18}-PEO14K-C_{18}	triblock	14.8	1.05	163	14.3
C_{18}-PEO30K-C_{18}	triblock	27.9	1.09	342	30.0
C_{18}-PEO47K-C_{18}	triblock	41.0	1.21	531	46.7
C_{18}-PEO94K-C_{18}	triblock	86.2	1.31	1062	93.5
C_{14}-PEO105K-C_{14}	triblock	83.6	1.21	1195	105
C_{22}-PEO50K-C_{22}	triblock	57.4	1.28	563	49.5
C_{22}-PEO93K-C_{22}	triblock	80.7	1.35	1060	93.3
C_6(PEO44K-C_{22})$_3$	three-arm star	126	1.37	1002	132
C_6(PEO90K-C_{22})$_3$	three-arm star	143	1.35	2050	270

[a] Determined by SEC (polystyrene calibration). [b] Mole ratio of ethylene oxide repeat units to alkyl end groups as determined by ^{1}H NMR spectroscopy. [c] Number-average molecular weight of the PEO segment assuming exactly two end groups per chain for the triblocks and three end groups per chain for the three-arm star blocks.

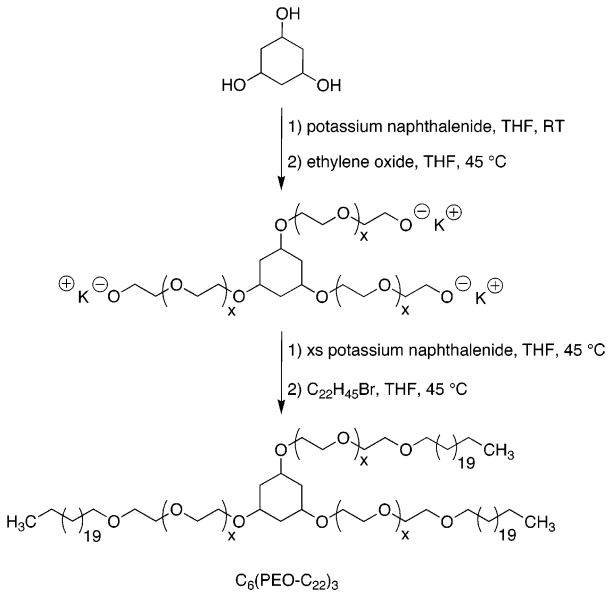

Figure 3. Synthesis of C_6(PEO-C_{22})$_3$ star block copolymers.

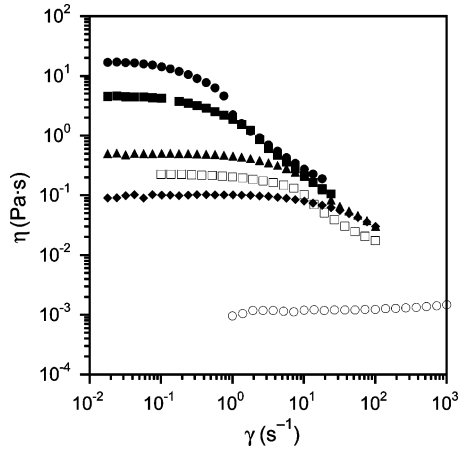

Figure 4. Shear rate dependent viscosity for a 1 wt % CTAT solution (open squares), a 0.1 wt % C_{18}-PEO94K-C_{18} solution (open circles), and aqueous mixtures containing 1 wt % CTAT and 0.1 wt % C_{18}-PEO94K-C_{18} (filled circles), C_{18}-PEO47K-C_{18} (filled squares), C_{18}-PEO30K-C_{18} (filled triangles), or C_{18}-PEO14K-C_{18} (filled diamonds).

response of a 0.1 wt % solution of C_{18}-PEO94K-C_{18} accurately due to its extremely low viscosity. Upon addition of 0.1 wt % C_{18}-PEO94K-C_{18} to the 1 wt % CTAT solution, the elastic modulus of the mixture was 1−3 orders of magnitude higher than the pristine CTAT solution, as shown in Figure 6. Furthermore, τ_R increased to about 1 s for this solution. These results are consistent with the steady flow viscosity behavior of the same solutions, in that the mixture of WLMs and HMPs

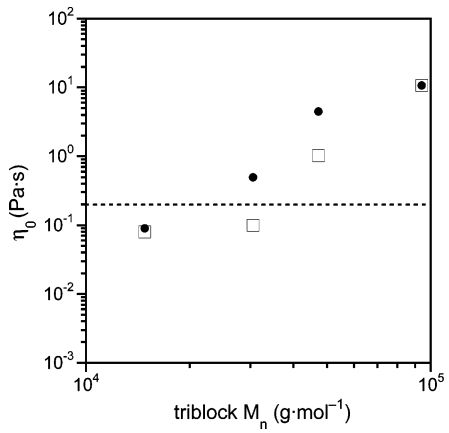

Figure 5. Dependence of η_0 on the molecular weight of the C_{18}-PEO-C_{18} triblock copolymers for solutions containing 1 wt % CTAT and 0.1 wt % C_{18}-PEO-C_{18} (filled circles). Analogous data for solutions containing constant sticker concentration (ca. 0.02 mM) is also presented (open squares). η_0 for a 1 wt % CTAT solution is indicated by a dashed line, and η_0 for a 0.1 wt % C_{18}-PEO94K-C_{18} is 10^{-3} Pa·s.

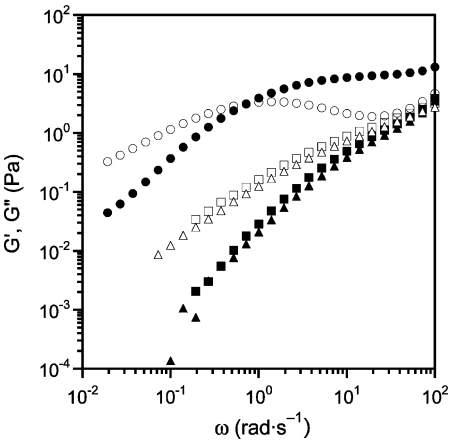

Figure 6. Dynamic elastic (G', filled symbols) and loss (G'', open symbols) moduli as a function of frequency for a 1 wt % CTAT solution (squares) and solutions containing 1 wt % CTAT and 0.1 wt % C_{18}-PEO94K-OH (triangles) or C_{18}-PEO94K-C_{18} (circles).

produces a greatly enhanced viscosity and longest relaxation time.

Figure 7 shows the dynamic response of C_{18}-PEO94K-C_{18}/1 wt % CTAT solutions as a function of triblock copolymer concentration, from 0.005% to 0.5% HMP. An evolution of the frequency-dependent moduli of these solutions as a function of polymer concentration can clearly be seen. By 0.05% HMP a distinct plateau emerges in G' at higher frequencies, and the plateau value increases with further addition of HMP. The values of τ_R for these solutions, although somewhat scattered, also increase as the hydrophobic sticker concentration increases.

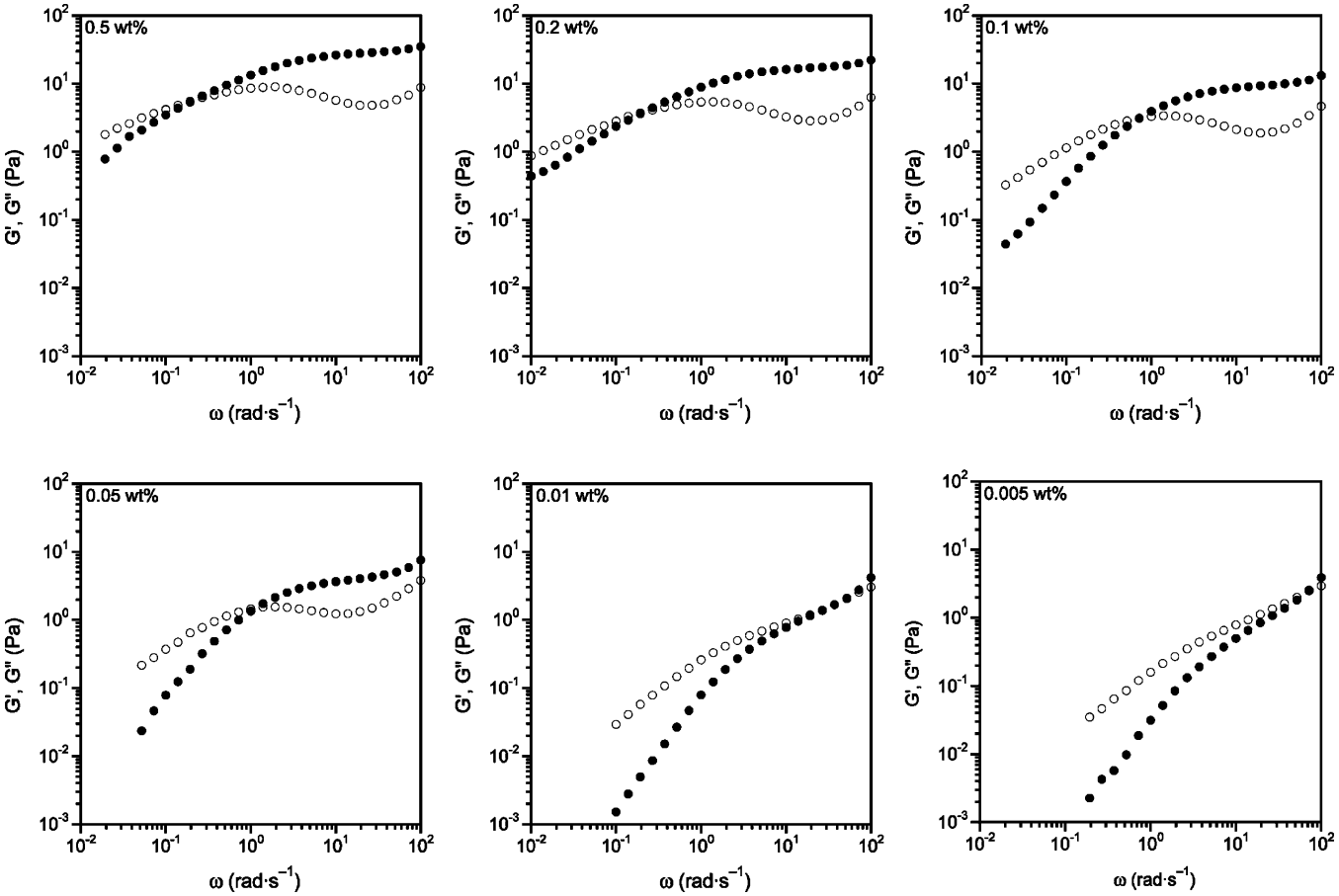

Figure 7. Dynamic elastic (G', filled circles) and loss (G'', open circles) moduli for solutions containing 1 wt % CTAT and C_{18}-PEO94K-C_{18} as a function of frequency (ω) at various C_{18}-PEO94K-C_{18} concentrations (indicated in the upper left-hand corner of each plot).

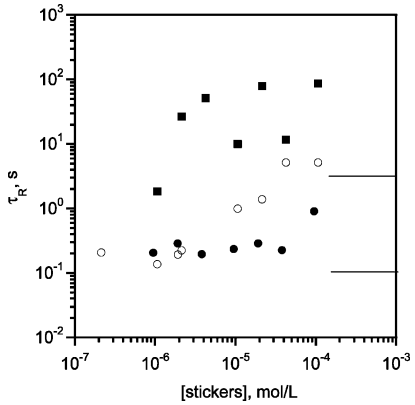

Figure 8. Dependence of τ_R on the concentration of hydrophobic stickers in solutions containing 1 wt % CTAT and 0.1 wt % C_{14}-PEO105K-C_{14} (filled circles), C_{18}-PEO94K-C_{18} (open circles), or C_{22}-PEO93K-C_{22} (filled squares). The line segments correspond to relative estimates of the sticker pullout time for the C_{14} and C_{18} systems based on a limiting τ_R for the C_{22} case of 100 s.

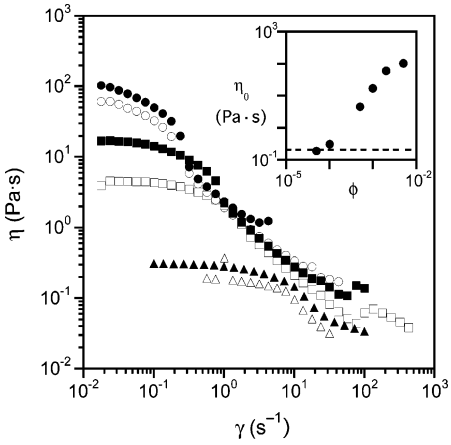

Figure 9. Shear rate dependent viscosity for solutions containing 1 wt % CTAT and C_{18}-PEO94K-C_{18} as a function of C_{18}-PEO94K-C_{18} concentration: 0.5 wt % (filled circles), 0.2 wt % (open circles), 0.1 wt % (filled squares), 0.05 wt % (open squares), 0.01 wt % (filled triangles), 0.005 wt % (open triangles). Inset: the zero shear viscosity for these solutions as a function of polymer weight fraction (ϕ). The zero shear viscosity for a 1 wt % CTAT solution is indicated as a dashed horizontal line.

These values are plotted separately in Figure 8 as open circles, and there is some suggestion that for each sticker length (see below) the relaxation time approaches a fixed value at high concentrations. The line segments in the plot are simple estimates of the relative sticker pullout times, to be discussed subsequently.

This behavior is also manifest in the steady shear behavior of these solutions as a function of polymer concentration (Figure 9); the crossover shear rate from Newtonian to shear thinning behavior generally tracks with the inverse of the characteristic relaxation time (i.e., the longer the relaxation time, the smaller the crossover shear rate). The inset of Figure 9 shows the change in η_0 with polymer concentration.

The dependence of the characteristic relaxation time on the PEO midblock molecular weight for the 0.1 wt % C_{18}-PEO-C_{18}/1 wt % CTAT solutions was also evaluated (Figure S1 of Supporting Information) and is summarized in Figure 10. As with the zero shear viscosity data (Figure 5), τ_R generally increases with the molecular weight of the PEO midblock.

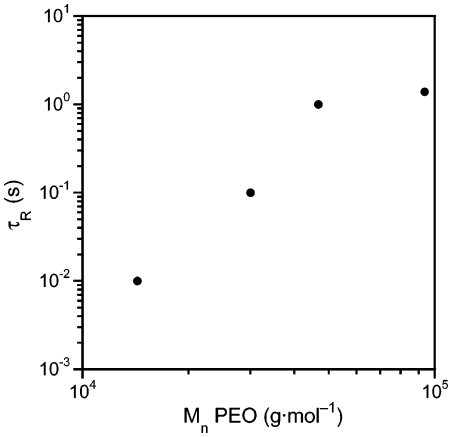

Figure 10. Dependence of the PEO midblock molecular weight on τ_R for 1 wt % CTAT/0.1 wt % C_{18}-PEO-C_{18} mixtures.

However, the difference in τ_R between the C_{18}-PEO47K-C_{18} and the C_{18}-PEO94K-C_{18} containing solutions is minimal, suggesting a possible saturation of the effect.

The dramatic influence of the hydrophobic sticker length at constant PEO midblock molecular weight on the dynamic response of 0.1 wt % C_n-PEO10^2K-C_n/1 wt % CTAT solutions is shown in Figure 11. A sample containing C_{14}-PEO105K-C_{14} behaved as a viscous solution (the dynamic response was essentially identical to the 1 wt % CTAT solution alone, see Figure 6), the C_{18}-PEO94K-C_{18} containing sample is a viscoelastic liquid (as discussed above), and the C_{22}-PEO93K-C_{22} sample gave a gel with a frequency-independent G' over the frequency range investigated (these C_{22}-PEO93K-C_{22} containing samples also passed the "vial inversion test" and did not flow over extended periods of time under the influence of gravity).[66] As for the 0.1 wt % C_{18}-PEO94K-C_{18}/1 wt % CTAT solutions, the dynamic responses of the mixtures containing C_{14}-PEO105K-C_{14} and the mixtures containing C_{22}-PEO93K-C_{22} were evaluated over a range of polymer concentrations (Figures S2 and S3). The characteristic relaxation times for all the mixtures are collected in Figure 8. In all the solutions, τ_R increases with increasing sticker concentration. However, triblock copolymers containing the C_{22} hydrophobes are much more effective at increasing the viscosity of the 1 wt % CTAT solutions compared to their C_{14} and C_{18} analogues.

Using model three-arm star block copolymers, we examined the influence of chain architecture on the viscoelastic properties of their aqueous mixtures with 1 wt % CTAT. The dynamic responses of 0.1 wt % C_6(PEO44K-C_{22})$_3$ or C_6(PEO90K-C_{22})$_3$ mixtures with 1 wt % CTAT at 25 °C are collected in Figures S4 and S5, respectively. Generally, the behavior of G' and G'' for these solutions was similar to that of the triblock C_{22}-PEO93K-C_{22} containing mixtures (Figure S3). To illustrate this, Figure 12 shows G' and G'' as a function of frequency for three solutions, one linear and two star HMPs, containing an approximately constant concentration of C_{22} hydrophobes ([C_{22}] $\approx$ 0.02 mM). Qualitatively, these solutions behave in a nearly identical manner, forming well-defined gels.

Discussion

The model HMPs used in this study were designed to allow for systematic variation of molecular weight, sticker size, and polymer architecture. PEO is a prototypical water-soluble polymer, and the linear alkyl end groups are analogous to the types of stickers used in other, less well-defined HMPs. The anionic polymerization method employed allowed for the synthesis of these materials with controlled molecular weights and narrow molecular weight distributions. Although there other wormlike micelle forming surfactants are available (e.g., EHAC), we focused our attention on the relatively well-characterized surfactant CTAT due to its documented ability to form wormlike micelles in dilute aqueous solution.

A 1 wt % CTAT solution shows the expected Newtonian behavior at low shear rates and shear thinning at high shear rates. The dynamic response of a 1 wt % CTAT solution is characterized by a Rouse-like spectrum of relaxation times, as expected for a weakly overlapping solution of long flexible chains, with a well-defined longest relaxation time τ_R. In all cases, adding low concentrations of a PEO molecule between about 10 and 100 kg mol^{-1} with only one sticker (i.e., the diblock architecture) led to no significant change (or a slight reduction) in both the zero shear viscosity and the characteristic relaxation time as compared to the pure CTAT solution, as exemplified in Figure 6. This is consistent with the idea that one hydrophobic sticker per polymer chain does not considerably perturb the wormlike chains formed by the CTAT surfactant molecules; we envision intercalation of the sticker into one of the worms, leaving a dangling PEO chain only decorating the micelle surface and not significantly influencing the dynamics of the system (e.g., breaking time, entanglement length, or reptation time of the micelles). The modest reduction in viscosity may reflect that the intercalated diblock actually stabilizes the end-cap of a WLM, thereby slightly reducing the average length of the WLMs.

In contrast to the diblocks, addition of low levels of C_n-PEO-C_n triblocks to the 1 wt % CTAT solution resulted in orders-of-magnitude increases in both η_0 and τ_R, depending on the exact molecular weight of the PEO midblock and concentration of the HMP. Using a 14.3 kg mol^{-1} PEO midblock at 0.1 wt % resulted in a modest decrease in η_0 compared to the pure CTAT solution, whereas a 94 kg mol^{-1} midblock led to a 2 order of magnitude increase in η_0. A simple interpretation of this behavior is that once the PEO midblocks are long enough, the hydrophobic stickers on each end can "cross-link" two wormlike micelles, thus retarding their dynamic response at low shear rates. (This is not unlike the cross-linking of linear polymers with the notable exception that the worms have a characteristic breaking time, and there is presumably a characteristic sticker/cross-link pullout time.) We propose that at lower PEO midblock molecular weights the distance between two end stickers is not sufficient to span two separate worms and both stickers tend to intercalate into one worm, and thus this system behaves essentially like a diblock (albeit with a looped PEO conformation). Note that we expect most stickers to participate in "flowerlike" micelles formed with other HMPs in the absence of CTAT[67] and that there is some combination of intercalation into wormlike micelles and flowerlike micelles in the solution mixtures. It is important to emphasize that in all the solutions examined the concentration of HMP is below its overlap concentration, and thus the enhanced viscoelastic response must arise from the combination of WLM and HMP. Furthermore, the HMP concentration is below that at which the HMP themselves would gel, and possibly induce phase separation, as documented by Russel and co-workers.[67] Confirming this expectation, all of the samples examined here were optically clear.

For the C_{18}-PEO14K-C_{18} and C_{18}-PEO94K-C_{18} samples we calculate mean end-to-end distances of about 14 and 42 nm, respectively, using light scattering data for PEO homopolymers in water (at 30 °C).[68] On the basis of previous reports,[29] we can anticipate a "mesh size" ξ for the 1% CTAT solution to be

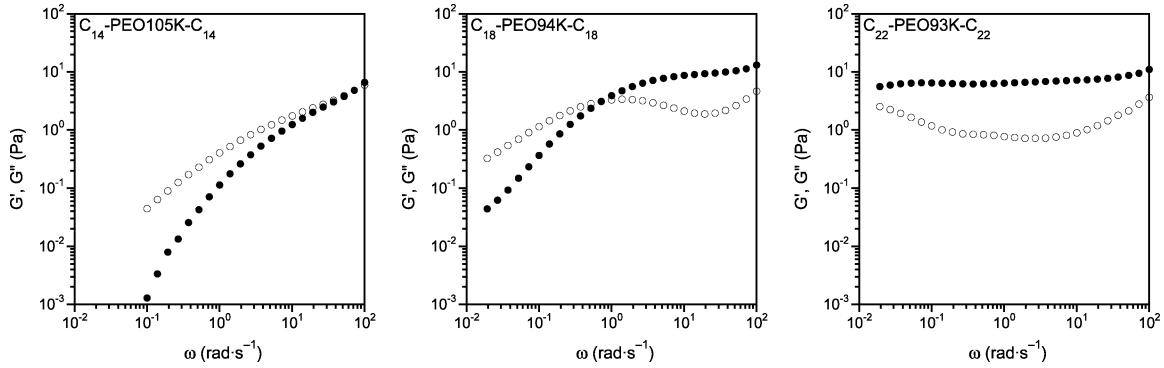

Figure 11. Dynamic elastic (filled circles) and loss (open circles) moduli for 1 wt % CTAT solutions containing 0.1 wt %: C_{14}-PEO105K-C_{14}, C_{18}-PEO94K-C_{18}, or C_{22}-PEO93K-C_{22}.

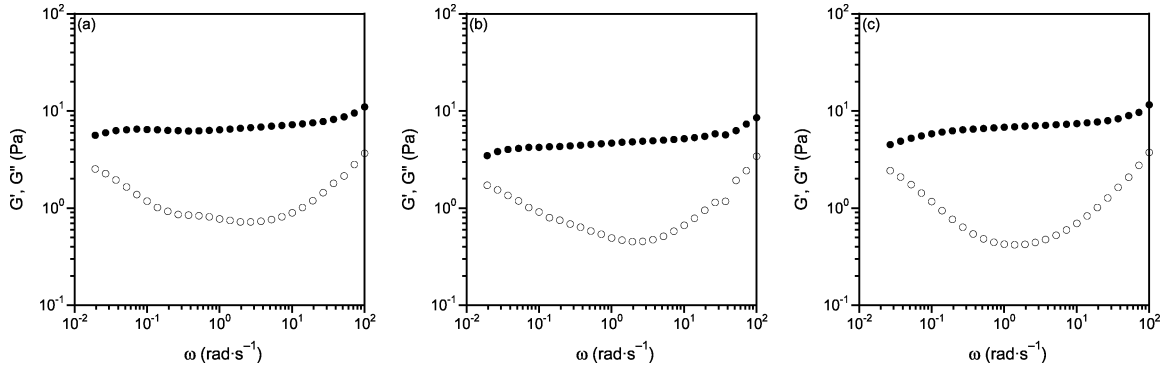

Figure 12. Dynamic elastic (G', filled circles) and loss (G'', open circles) moduli for 1 wt % CTAT solutions containing (a) 0.1 wt % C_{22}-PEO93K-C_{22}, (b) 0.1 wt % C_6(PEO44K-C_{22})$_3$, or (c) 0.2 wt % C_6(PEO90K-C_{22})$_3$.

on the order of 100 nm; similar values will be extracted below from data on the observed gels. Specifically, a plateau modulus of about 5 Pa implies an average mesh size of about 94 nm, as $G' \approx kT/\xi^3$. Thus, the mesh size is consistently larger than average HMP dimensions. As summarized in Figure 5, increasing the molecular weight of the triblocks leads to an increase in the probability that one molecule spans two worms. Since the end-to-end distance increases as (essentially) the square root of the molecular weight, the dramatic influence of interconnecting the worms on the viscosity is reflected in the strong dependence of η_0 with the triblock molecular weight.

The increases observed in η_0 are also consistent with the increases in characteristic relaxation time observed with increasing triblock molecular weight (at constant sticker concentration) for solutions containing 1 wt % CTAT and 0.1 wt % C_{18}-PEO-C_{18}. Both τ_R and η_0 scale with the triblock molecular weight to about the one-third power (Figure 10). Furthermore, the higher the C_{18} sticker concentration, the longer the characteristic relaxation time of the admixtures (Figures 7 and 8). Similarly, η_0 increases monotonically with sticker (polymer) concentration for the C_{18}-PEO94K-C_{18} system, as shown in Figure 9. Again, these data support the idea that the end stickers interconnect the worms leading to a significant perturbation in their relaxation characteristics; the more interconnected the worms are, the slower the dynamics and the higher the viscosity at low shear rates. We feel a reasonable explanation for the increase in the relaxation time for the solutions is due mainly to the increase in relaxation time for the "cross-linked" wormlike micelles; addition of a low concentration of stickers probably does not influence the breaking time of the wormlike micelles since there are about 1000 times more surfactant molecules than stickers in a typical sample ([CTAT] $\approx$ 20 mM and [stickers] $\approx$ 0.02 mM for a 1 wt % CTAT/0.1 wt % C_{18}-PEO94K-C_{18} mixture).

The dramatic effect of sticker length on the relaxation time is evident in Figures 8 and 11 and highlights another important time scale in the relaxation dynamics of these systems: the frequency of sticker pullout from the WLMs. At equivalent sticker concentrations, the C_{22} stickers on a C_{22}-PEO10^2K-C_{22} triblock result in gelation of the 1 wt % CTAT solution ($\tau_R >$ ca. 10 s), whereas C_{14} stickers have very little influence on the rheological properties compared to the 1 wt % CTAT solution. A straightforward interpretation of this phenomenon is that the pullout time for C_{14} stickers is very short or comparable to the WLM relaxation time, and the pullout time for C_{22} stickers is very long compared to the WLM relaxation time; the C_{14} stickers are too dynamic to "fix" the wormlike micelles, and the C_{22} stickers act effectively as cross-links. This analysis is consistent with the data shown in Figure 8. In the C_{14} and C_{18} samples, the relaxation time increases monotonically with sticker concentration but may show evidence of a plateau at higher concentrations. For C_{22} the plateau is clear; once the concentration of C_{22} stickers reaches about 5×10^{-6} M, the relaxation time remains essentially constant upon further increases in concentration (all samples above this concentration behave like gels). The concentration of stickers is roughly equal to 5 stickers per 10^6 nm^3. This volume corresponds to approximately the calculated mesh length (94 nm) cubed, and we estimate about the same number of worms as stickers in this volume. This is consistent with the interconnected worm model given that the gel point should occur at about one sticker per worm.

On the basis of the work of Meng and Russel,[69] we may estimate the ratio of sticker pullout times for the three stickers. Specifically, they suggest that the activation energy for sticker pullout increases by $0.86kT$ per CH_2 unit. This, in turn, implies that if the saturation value of τ_R (i.e., corresponding to the inverse of the pullout "rate constant") in Figure 8 of about 100 s is due to the pullout of C_{22} stickers, then the corresponding

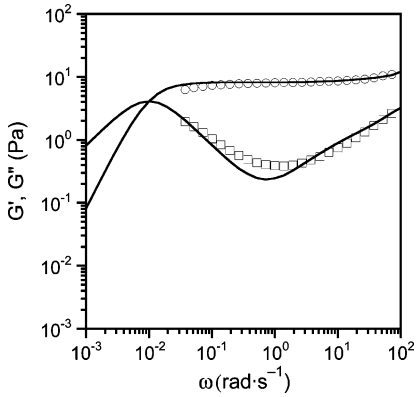

Figure 13. Dynamic elastic (G', open circles) and loss (G'', open squares) for 1 wt % CTAT solutions containing 0.1 wt % C_6(PEO90K-C_{22})$_3$. The solid line is the sum of a single Maxwell element plus the bare 1% CTAT solution response shown in Figure 6. The low-frequency response of the CTAT solution was estimated by assuming terminal behavior.

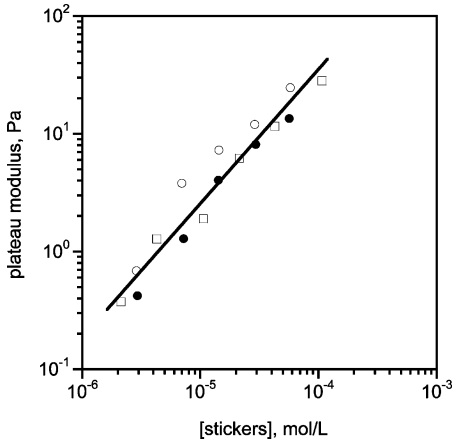

Figure 14. Plateau modulus (taken as the value of G' at the frequency where G'' has a local minimum) as a function of sticker concentration for the C_{22} sticker HMPs that form gels when mixed with 1 wt % CTAT: C_6(PEO44K-C_{22})$_3$, filled circles; C_6(PEO90K-C_{22})$_3$, open circles; C_{22}-PEO93K-C_{22}, open squares. The straight line, drawn to guide the eye, indicates a linear dependence.

"saturation" value of the longest relation time should be reduced by a factor of 30 ($e^{4\times0.86}$) for C_{18} and almost 1000 ($e^{8\times0.86}$) for C_{14}. These two estimates based on the experimental value of τ_R for the C_{22} case are in fair agreement with the data in Figure 8, as indicated by the two horizontal line segments, thereby supporting the overall interpretation. We may push this analysis one step further to estimate the actual value of the pullout time for the C_{22} sticker by approximating the "attempt time" (i.e., the inverse of the preexponential or frequency factor for this activated process). We suspect that this should correspond to some internal modes of the PEO chain to which the sticker is attached. As an upper bound we can estimate the longest (Zimm) relaxation time of this 100K midblock as $8\pi\eta R_g^3/kT \approx 30\ \mu$s, which would give a maximum pullout time of about 5000 s ($= 30 \times 10^{-6}$ s/$e^{-22\times0.86}$). A maximum pullout time of 100 s (see Figure 8) would imply an attempt time of about 1 μs, suggesting that motions of smaller subsections of the PEO midblocks are implicated. In any event, this analysis at least establishes the plausibility of the interpretation that the observed relaxation time is dictated by the sticker pullout.

For samples that show a clear gel-like response, it is actually possible to provide a good description of the viscoelastic response in a very simple way. This is illustrated in Figure 13 for the mixture with 0.1 wt % C_6(PEO90K-C_{22})$_3$. The sum of a Maxwell model with one relaxation time (100 s) and a high-frequency modulus of 8.2 Pa (the value of G' corresponding to the local minimum of G'') and the response of the bare 1% CTAT solution (see Figure 6) gives a remarkably good fit to the experimental data. The CTAT solution's response accounts for the rise in both moduli at higher frequencies. In short, these mixtures can be described as transient networks with a well-defined flow time and with the internal modes of the network strands being the same as those of the WLMs in solution. It is worth emphasizing that this Maxwell response does not have the same origin as that in the Cates model of living polymers.[70] That model applies to well-entangled systems with stress relaxation due to a combination of chain reptation and breakage. In our mixtures the WLMs are not entangled and therefore do not reptate.

All the samples containing three-arm star HMPs, and those with the highest molecular weight linear triblock, with C_{22} stickers exhibit well-defined plateau moduli (again, taken as the value of G' at the frequency where G'' has a local minimum). The linear dependence of modulus on concentration is shown in Figure 14. If a fixed fraction of stickers are intercalated into WLMs (the rest presumably being associated in HMP micelles), then the number of cross-links should increase linearly with concentration. This would lead to a linear decrease in the average "molecular weight" of the WLM between cross-links and the concomitant linear increase in modulus, as observed. For both the triblocks with C_{22} stickers (Figure 8) and the star polymers with C_{22} stickers, τ_R appears to approach a value near 100 s. This apparent saturation of the relaxation time is also consistent with the hypothesis that this time is dictated by sticker pullout.

Conclusions

In conclusion, we have demonstrated that the addition of very small amounts of model hydrophobically end-capped poly(ethylene oxide)s to a solution containing wormlike micelles (formed from a low-molecular-weight surfactant) leads to a substantial increase in both the linear viscoelastic moduli and steady shear viscosity of these ternary mixtures. Large enhancements in the viscoelastic response of these mixtures were observed upon increasing hydrophobe length at fixed polymer molecular weight and concentration and by increasing the poly(ethylene oxide) molecular weight at fixed concentration. At long enough PEO chain lengths, we propose that the hydrophobic stickers on each end can "cross-link" two wormlike micelles, thus retarding their dynamic response at low shear rates. Furthermore, the increase in the observed relaxation times is a direct consequence of the increase in relaxation time for the "cross-linked" wormlike micelles and is likely not due to any changes in their breaking time. We also found that the sticker length plays a significant role in the overall dynamics of the system. The pullout time for a sticker is directly related to its length, and we suggest that the pullout time for C_{14} stickers is very short and comparable to the WLM relaxation time and the pullout time for C_{22} stickers is very long compared to the WLM relaxation time. At equivalent sticker concentrations, the C_{22} stickers on a C_{22}-PEO10^{2}K-C_{22} triblock result in effective gelation of 1 wt % CTAT solutions, whereas C_{14} stickers have very little influence on the rheological properties. As a result, we conclude that the C_{14} stickers are too dynamic to "fix" the wormlike micelles, but the C_{22} stickers act quite effectively as cross-links. Finally, modeling of mixtures that form gels led us to the conclusion that these systems can be described as transient networks with a well-defined flow time and with the internal

modes of the network strands being the same as those of the WLMs in solution. Thus, the most straightforward mechanism that is consistent with our observed results is that intercalation of the hydrophobic stickers into the wormlike micelles physically cross-links the system.

Experimental Details

Materials. All commercial solvents and chemicals were used as received with the following exceptions. Tetrahydrofuran (THF), when used as a polymerization solvent, was purified by passing through an activated alumina column using a home-built solvent purification system. Ethylene oxide (Aldrich, 99.5%) was vacuum-distilled twice from *n*-butyl lithium after stirring in a sealed flask at 0 °C for 1 h. $C_{18}H_{37}Br$ and $C_{22}H_{45}Br$ were recrystallized in ethyl acetate and dried overnight under vacuum.

Synthesis of AB Diblock and ABA Triblock Copolymers. A typical polymerization procedure is described below. The polymerizations were performed in a 2 L round-bottom glass reactor equipped with a magnetic stir bar, four Teflon bushings fitted with Viton O-rings, and a Y-connector with three ports (Ar/vacuum manifold, manometer, and septum) which was charged with $C_{22}H_{45}$-OH and evacuated under dynamic vacuum for 1 h. The flask was then back-filled with Ar, setting the pressure to 2−3 psig. THF was added to the flask, and the solution was stirred until the $C_{22}H_{45}$-OH completely dissolved. A solution of a potassium naphthalenide was prepared in a graduated cylinder fitted with a Teflon valve and side hose adapter. The deep green potassium naphthalenide solution was stirred under argon overnight. The solution of $C_{22}H_{45}$-OH was slowly titrated with the freshly prepared potassium naphthalenide solution until a light green solution persisted at least 10 min at room temperature. The EO was added in one portion to the solution. The reaction mixture became colorless immediately. The reaction was heated to 40−45 °C and stirred at least 12 h. For the AB diblock samples, the polymerization was then terminated with acidic methanol. In the case of the ABA triblock samples, after complete conversion of the ethylene oxide, a small quantity of potassium naphthalenide solution was added to confirm all hydroxy groups were converted to the potassium alkoxide analogs. $C_{22}H_{45}Br$ was added to end-cap the polymer. The end-capping reaction was performed at 45 °C for 2 h. Upon completion, the reactor was cooled to room temperature and precipitated into hexanes. The recovered polymer was redissolved to dichloromethane and washed by DI water three times, followed by pouring into hexanes again. This process was repeated a total of three times. The recovered polymer was dried in a vacuum overnight at room temperature.

Synthesis of Three-Arm Star Block Copolymers. The polymerization procedure was the same as for the ABA triblock copolymers, except trifunctional alcohol (1,3,5-cyclohexanetriol) was used as the initiating species.

Sample Preparation. The CTAT/polymer mixture solutions were prepared by mixing appropriate solid CTAT and solid polymer with pure water at 60 °C with vigorous stirring for 24 h. The sample were cooled to room temperature slowly and left for to equilibrate at room temperature for 24 h.

Rheological Measurements. Dynamic and steady rheological measurements were carried using a Rheometrics RFS II rheometer equipped with a cup-and-bob geometry (34 mm cup and 32 mm bob). The temperature was controlled using a Rheometrics environmental circulater (fluid circulating system). The dynamic frequency spectra were obtained in the linear viscoelastic regime, as determined by dynamic stress sweep experiments. The frequency was varied between 10^{-2} and 10^{2} rad s^{-1}. Steady-state measurement were performed under controlled shear rate by using same geometry with optimized relaxation time (10−300 s, depending on the sample). The shear rate was varied between 10^{-2} and 10^{2} s^{-1}. In the all experiments, the samples were equilibrated for at least 30 min at each temperature. A plastic cover with wet sponge was used to help prevent water evaporation from the samples.

Acknowledgment. This work was supported by Schlumberger and in part by the MRSEC Program of the National Science Foundation under Award DMR-0212302. We also thank Dr. Alejandro Pena for fruitful discussions.

Supporting Information Available: Figures S1−S5. This material is available free of charge via the Internet at http://pubs.acs.org.

References and Notes

(1) Magid, L. J. *J. Phys. Chem. B* **1998**, *102*, 4064.
(2) Walker, L. M. *Curr. Opin. Colloid. Interface Sci.* **2001**, *6*, 451.
(3) Candau, S. J.; Hirsch, E.; Zana, R. *J. Phys. (Paris*) **1984**, *45*, 1263.
(4) Candau, S. J.; Hirsch, E.; Zana, R. *J. Colloid Interface Sci.* **1985**, *105*, 521.
(5) Cates, M. E.; Candau, S. J. *J. Phys.: Condens. Matter* **1990**, *2*, 6869.
(6) Wan, L. S. C. *J. Pharm. Sci.* **1966**, *55*, 1395.
(7) Brown, W.; Johansson, K.; Aimgren, M. *J. Phys. Chem.* **1989**, *93*, 5888.
(8) Imae, T.; Kohsaka, T. *J. Phys. Chem.* **1992**, *96*, 10030.
(9) Kaler, E. W.; Herrington, K. L.; Murthy, A. K.; Zasadzinski, J. A. N. *J. Phys. Chem*. **1992**, *96*, 6688.
(10) Hassan, P. A.; Valaulikar, B. S.; Manohar, S.; Kern, F.; Bourdieu, L.; Candau, S. *Langmuir* **1996**, *12*, 4350.
(11) Carver, M.; Smith, T. L.; Gee, J. C.; Delichere, S.; Caponetti, E.; Magid, L. *Langmuir* **1996**, *12*, 691.
(12) Bachofer, S. J.; Simonis, U. *Langmuir* **1996**, *12*, 1744.
(13) Koehler, R. D.; Raghavan, S. R.; Kaler, E. W. *J. Phys. Chem. B* **2000**, *104*, 11035.
(14) Soltero, J. F. A.; Puig, J. E.; Manero, O.; Schulz, P. C. *Langmuir* **1995**, *11*, 3337.
(15) Soltero, J. F. A.; Puig, J. E.; Manero, O. *Langmuir* **1996**, *12*, 2654.
(16) Soltero, J. F. A.; Bautista, F.; Puig, J. E.; Manero, O. *Langmuir* **1999**, *15*, 1604.
(17) Raghavan, S. R.; Kaler, E. W. *Langmuir* **2001**, *17*, 300.
(18) Croce, V.; Cosgrove, T.; Maitland, G.; Hughes, T.; Karlsson, G. *Langmuir* **2003**, *19*, 8536.
(19) Kalur, G. C.; Frounfelker, B. D.; Cipriano, B. H.; Norman, A. I.; Raghaven, S. R. *Langmuir* **2005**, *21*, 10998.
(20) Gerber, M. J.; Kline, S. R.; Walker, L. M. *Langmuir* **2004**, *20*, 8510.
(21) Hubbard, F. P.; Santonicola, G.; Kaler, E. W.; Abbott, N. L. *Langmuir* **2005**, *21*, 6131.
(22) Granek, R.; Cates, M. E. *J. Chem. Phys.* **1992**, *96*, 4758.
(23) Kubowicz, S.; Thünemann, A. F.; Weberskirch, R.; Möhwald, H. *Langmuir* **2005**, *21*, 7214.
(24) Shikata, T.; Hirata, H. *Langmuir* **1987**, *3*, 1081.
(25) Shikata, T.; Hirata, H. *Langmuir* **1989**, *5*, 398.
(26) Lu, B.; Li, X.; Scriven, L. E.; Davis, H. T.; Talmon, Y.; Zakin, J. L. *Langmuir* **1998**, *14*, 8.
(27) Almgren, M.; Garamus, V. M. *J. Phys. Chem. B* **2005**, *109*, 11348.
(28) Clausen, T. M.; Vinson, P. K.; Minter, J. R.; Davis, H. T.; Talman, Y.; Miller, W. G. *J. Phys. Chem.* **1992**, *96*, 474.
(29) Schubert, B. A.; Kaler, E. W.; Wagner, N. J. *Langmuir* **2003**, *19*, 4079.
(30) Gamez-C, R.; Berret, J. −F.; Walker, L. M.; Oberdisse, J. *Langmuir* **1999**, *15*, 6755.
(31) Granek, R. *Langmuir* **1994**, *10*, 1627.
(32) Raghavan, S. R.; Edlund, H.; Kaler, E. W. Raghavan, S. R.; Kaler, E. W. *Langmuir* **2002**, *18*, 1056.
(33) Kim, B.-S.; Hong, D.-J.; Bae, J.; Lee, M. *J. Am. Chem. Soc.* **2005**, *127*, 16333.
(34) Sakai, H.; Orihara, Y.; Kodashima, H.; Matsumura, A.; Ohkubo, T.; Tsuchiya, K.; Abe, M. *J. Am. Chem. Soc*. **2005**, *127*, 13454.
(35) Hassan, P. A.; Raghaven, S. R.; Kaler, E. W. *Langmuir* **2002**, *18*, 2543.
(36) Nakamura, K.; Shikata, T. *Macromolecules* **2004**, *37*, 8381.
(37) Yang, J. *Curr. Opin. Colloid Interface Sci.* **2002**, *7*, 276.
(38) Lee, J. H.; Gustin, J. P.; Chen, T.; Payne, G. F.; Raghavan, S. R. *Langmuir* **2005**, *21*, 26.
(39) Truong, M. T.; Walker, L. M. *Langmuir* **2000**, *16*, 7991.
(40) Hoff, E.; Nyström, B.; Lindman, B. *Langmuir* **2001**, *17*, 28.
(41) Winnik, F. M.; Regismond, S. T. A. *Colloids Surf., A* **1996**, *118*, 1.
(42) Kwak, J. C. T., Ed. *Polymers-Surfactants Systems;* Surfactant Science Sereis 77; Dekker: New York, 1998.
(43) Shashkina, J. A.; Philippova, O. E.; Zaroslov, Y. D.; Khokhlov, A. R.; Pryakhina, T. A.; Blagodatskikh, I. V. *Langmuir* **2005**, *21*, 1524.
(44) Couillet, I.; Hughes, T.; Maitland, G.; Candau, F. *Macromolecules* **2005**, *38*, 5271.
(45) Ryu, J-H.; Lee, M. *J. Am. Chem. Soc*. **2005**, *127*, 14170.
(46) Alami, E.; Almgren, M.; Brown, W. *Macromolecules* **1996**, *29*, 2229.
(47) Nicolai, T.; Benyahia, L. *Macromolecules* **2005**, *38*, 9794.

(48) Tanaka, F.; Edwards, S. F. *Macromolecules* **1992**, *25*, 1516.
(49) Abrahmsen, A. S.; Alami, E.; Francois, J. *J. Colloid Interface Sci.* **1996**, *179*, 20.
(50) Beaudoin, E.; Borisov, O.; Lapp, A.; Francois, J. *Macromol. Symp.* **2002**, *189*, 89.
(51) Beaudoin, E.; Hiorns, R. C.; Francois, J. *Langmuir* **2003**, *19*, 2058.
(52) Beaudoin, E.; Gourier, C.; Hiorns, R. C.; Francois, J. *J. Colloid Interface Sci.* **2002**, *251*, 398.
(53) Annable, T.; Buscall, R.; Ettelaie, R.; Whittlestone, D. *J. Rheol.* **1993**, *37*, 695.
(54) Kaczmarski, J. P.; Glass, J. E. *Langmuir* **1994**, *10*, 3035.
(55) Lundberg, D. J.; Brown, R. G.; Glass, J. E.; Eley, R. R. *Langmuir* **1994**, *10*, 3027.
(56) Chassenieux, C.; Nicolai, T.; Durand, D. *Macromolecules* **1998**, *31*, 4035.
(57) Kaczmarski, J. P.; Glass, J. E. *Macromolecules* **1993**, *26*, 5149.
(58) Chassenieux, C.; Nicolai, T.; Durand, D. *Macromolecules* **1997**, *30*, 4952.
(59) Barmar, M.; Ribitsch, V.; Kaffashi, B.; Barikani, M.; Sarreshtehdari, Z.; Pfragner, J. *Colloid Polym. Sci.* **2004**, *282*, 454.
(60) Beaudoin, E.; Borisov, O.; Lapp, A.; Billon, L.; Hiorns, R. C.; Francois, J. *Macromolecules* **2002**, *35*, 7436.
(61) Serero, Y.; Aznar, R.; Porte, G.; Berret, J. -F.; Calvet, D.; Collet, A.; Viguier, M. *Phys. Rev. Lett.* **1998**, *81*, 5584.
(62) Indei, T.; Koga, T.; Tanaka, F. *Macromol. Rapid Commun.* **2005**, *26*, 701.
(63) Tam, K. C.; Jenkins, R. D.; Winnik, M. A.; Bassett, D. R. *Macromolecules* **1998**, *31*, 4149.
(64) Yekta, A.; Xu, B.; Duhamel, J.; Adiwidjaja, H.; Winnik, M. A. *Macromolecules* **1995**, *28*, 956.
(65) Hillmyer, M. A.; Bates, F. S. *Macromolecules* **1996**, *29*, 6994−7002.
(66) It does appear that the elastic and loss moduli for the "gels" we observed in this study will intersect at lower frequencies. Therefore, the relaxation time for these samples is likely not infinite, leading to a liquidlike response at very long times.
(67) Pham, Q. T.; Russel, W. B.; Thibeault, J. C.; Lau, W. *Macromolecules* **1999**, *32*, 2996.
(68) Devanand, K.; Selser, J. C. *Macromolecules* **1991**, *24*, 5943.
(69) Meng, X.-X.; Russel, W. B. *J. Rheol.* **2006**, *50*, 189.
(70) (a) Cates, M. E. *Macromolecules* **1988**, *21*, 256−259. (b) Cates, M. E. *Macromolecules* **1987**, *20*, 2289−2296.

MA062428+